Journal of Advances in Mathematics and Computer Science

31(3): 1-25, 2019; Article no.JAMCS.43089
ISSN: 2456-9968
(Past name: British Journal of Mathematics & Computer Science, Past ISSN: 2231-0851)

MHD Maxwell Reactive Flow with Velocity Slip Over a Stretching Surface with Prescribed Heat Flux in the Presence of Thermal Radiation in a Porous Medium

I. G. Baoku[1*] and K. I. Falade[2]

[1]Department of Mathematical Sciences, Federal University, Dutsin-Ma, Katsina State, Nigeria.
[2]Department of Mathematics, Kano University of Science and Technology, Wudil, Kano State, Nigeria.

Authors' contributions

This work was carried out in collaboration between the authors. Author IGB designed the study, performed the computational analysis, wrote the protocol and wrote the first draft of the manuscript. Author KIF managed the analyses of the study and the literature searches. Both authors read and approved the final manuscript.

Article Information

DOI: 10.9734/JAMCS/2019/v31i330116
Editor(s):
(1) Dr. Francisco Welington de Sousa Lima, Dietrich Stauffer Laboratory for Computational Physics, Departamento de Física, Universidade Federal do Piauí, Teresina, Brazil.
Reviewers:
(1) Zahir Shah, Ghandhara University of Science and Technology, Pakistan.
(2) Imdat Taymaz, Sakarya University, Turkey.
Complete Peer review History: http://www.sdiarticle3.com/review-history/43089

Original Research Article

Received: 25 April 2018
Accepted: 20 July 2018
Published: 28 March 2019

Abstract

This article is concerned with the study of heat and mass transfer of a MHD reactive flow of an upper-convected Maxwell fluid model over a stretching surface subjected to a prescribed heat flux with velocity slip effect in a Darcian porous medium in the presence of thermal radiation and internal heat generation/absorption. The basic boundary layer governing partial differential equations are transformed into a set of coupled ordinary differential equations, which are solved numerically using Runge-Kutta-Fehlberg integration scheme with shooting technique. The far field boundary conditions are asymptotically satisfied to support the accuracy of the numerical computations and the results obtained. The velocity, temperature and species concentration profiles are enhanced by increasing values of velocity slip parameter with Hartmann number, heat generation/absorption parameter and order of chemical reaction parameter respectively. Increments in the values of velocity slip parameter, Hartmann number, rate of chemical reaction parameter and Prandtl number boost the wall shear stress, dimensionless surface temperature is increased by increasing values of Deborah number, heat

**Corresponding author: E-mail: ibaoku@fudutsinma.edu.ng;*

generation/absorption and order of chemical reaction parameters while local rate of mass transfer is enhanced by increments in the values of Hartmann number, suction velocity, Darcian porous medium, rate of chemical reaction and velocity slip parameters. The presence of velocity slip on the flow distribution is found to be of great significance to the study.

Keywords: *Magnetohydrodynamics; stretching surface; thermal radiation; porous medium, Maxwell fluid; velocity slip; prescribed heat flux.*

1 Introduction

It is evident that several industrial fluids are non-Newtonian in their flow features. In a Newtonian fluid, the shear stress is directly proportional to the rate of shear strain, whereas the relationship between shear stress and the rate of shear strain is nonlinear in the case of a non-Newtonian fluid. Most of the particulate slurries such as china clay and coal in water; multiphase mixtures such as paints, synthetic lubricants, oil-water emulsions; biological fluids including blood at a low shear rate, synovial fluid, and saliva; and foodstuffs such as jams, jellies, soups, and marmalades are examples of non-Newtonian fluids. Due to the large variety of the non-Newtonian fluids, many models of these fluids exist. Maxwell model is one subclass of rate type of non-Newtonian fluids. This fluid model predicts the relaxation time effects which cannot be predicted by the differential-type non-Newtonian fluids. Maxwell fluid model is useful for polymers of low molecular weight. A review of non-Newtonian Maxwell fluid flow problems with heat and/or mass transfer may be found in many researchers [1-13].

The flow, heat and mass transfer due to stretching surfaces in non-Newtonian fluids are of significant practical interests because they occur in a number of manufacturing and engineering processes; for example, in the polymer industry when a polymer sheet is extruded continuously from a die, with tacit assumption that the sheet is inextensible. During its manufacturing process, a stretched sheet interacts thermally and mechanically with the ambient fluid. The thermal interaction is governed by the surface heat flux. This quantity can either be prescribed or it is the output of a process in which the surface temperature distribution has been prescribed. The cooling of a large metallic plate in a bath (electrolyte) is another problem belonging to this category. Other interesting applications of the flows due to stretching surface are in the continuous casting, glass blowing, wire drawing, spinning of fibres, paper production and hot rolling. However, in other real situations, one encounters the boundary layer flow over stretching sheets/surfaces. For instance, in a melt-spinning process, the extrudate is stretched into a filament or sheet while it is drawn from the die. Finally, this sheet solidifies while it passes through an effectively controlled cooling system in order to acquire the top grade property of the final product. One can refer to the following studies in references [14-21] on the flows of Maxwell fluid over stretching surfaces with heat and/or mass transfer phenomena.

Due to its important applications in industrial technology, the MHD study has considerable interest in the technical fields. These applications comprise MHD power generators, cooling of nuclear reactions, liquid metal flow control, biological transportation, high-temperature plasmas, micro MHD pumps, drying processes, solidification of binary alloy, etc. Shah et al. [22-23] has recently examined the electrical MHD and Hall current impact on micropolar nanofluid flow between rotating parallel plates; and a three dimensional non-Newtonian nanofluid flow with mass and heat transmission in a rotating frame in the existence of a magnetic field in which Hall current was taken into account respectively. Khater et al. [24] presented a weakly nonlinear theory of wave propagation in superposed fluids in the presence of a magnetic field. They examined the nonlinear evolution of Rayleigh-Taylor instability in three dimensions in the context of magnetohydrodynamics and performed a stability analysis of their solutions. The mass transfer of the steady two-dimensional magnetohydrodynamic boundary layer flow of an upper-convected Maxwell fluid past a porous shrinking sheet in the presence of chemical reaction was investigated by Hayat et al. [25]. They used homotopy analysis method (HAM) to obtain series solutions for the problem. Baoku et al. [26] studied the influence of magnetic field, third grade, partial slip and other thermophysical parameters on the steady flow, heat and mass transfer of viscoelastic third grade fluid past an infinite vertical insulated plate subject to suction across the boundary layer. It was concluded that the magnetic field strength was found to decrease with an increasing temperature distribution when the porous plate was insulated.

Olajuwon et al. [27] considered the hydromagnetic partial slip flow, heat and mass transfer of a third-grade non-Newtonian fluid over a vertical surface in the presence thermal radiation in an optically thick media through a porous medium. They employed the midpoint integration scheme alongside Richardson's extrapolation technique to obtain numerical solutions to the problem. The entropy generation in a magnetohydrodynamic flow and heat transfer of a Maxwell fluid was reported by Shateyi et al. [28]. They obtained the solutions to the problem using the spectral relaxation method. Liu and Guo [29] examined the magnetohydrodynamic flow of a generalized Maxwell fluid, induced by a moving plate where there is a second-order slip between the wall and the fluid. They pointed out that the velocity corresponding to flows with slip condition subjected to a magnetic field is lower than that with first-order slip condition. Gaffar et al. [30] analyzed the nonlinear, isothermal, steady-state, free convection boundary layer flow of an incompressible third-grade viscoelastic fluid past an isothermal inverted cone in the presence of magnetohydrodynamic, thermal radiation and heat generation/absorption. They employed the second-order accurate implicit finite-difference Keller-Box Method to obtain solutions for the transformed conservation equations of linear momentum, heat and mass subject to the realistic boundary conditions.

Many recent engineering processes occur at high temperatures. Therefore, the knowledge of radiation heat transfer besides the convective heat transfer plays very crucial roles and cannot be neglected. Gas turbines, nuclear power plants and several propulsion devices for missiles, satellites aircraft and space vehicles are few examples of such engineering areas involving thermal radiation. (see Eckert and Drake [31]). Many researches on influences of thermal radiation on viscous fluids over different surfaces have been conducted by Gorla [32], Raptis and Massalas [33], Pop et al. [34], Abdul Hakeem and Sathiyanathan [35], Hossain et al. [36], Hayat et al. [37] and Baoku et al. [38]. In the same vein, one can refer to the works of Gorla and Pop [39], Siddheshwar and Mahabaleshwar [40], Olajuwon and Baoku [41], Aliakbar et al. [42], Mushtaq et al. [43], Bilal et al. [44], Baoku and Fadare [45], Shah et al. [46], Ishaq et al. [47], Nasir et al. [48], Muhammad et al. [49] concerning the thermal radiation effects on Maxwell fluid and other non-Newtonian fluids.

Flows in porous media have gained the attention of many researchers because of their applications in astrophysics, geothermal and oil reservoir engineering. Flows involving viscous and non-Newtonian fluids have been studied extensively. One can make references to the works Vafai and Tien [50], Raptis [51], Ingham and Pop [52], Mohammadein and El-Amin [53], Vafai [54], Pop and Ingham [55], Ingham et al. [56], Ingham and Pop [57], Vafai [58], Nield and Bejan [59], Hayat et al. [60] and references therein concerning viscous and non-Newtonian flow through Darcian and non-Darcian porous media with different geometries for the flows. However, they are still open problems on flows in porous media with non-Newtonian fluid. Detailed discussions have been given in these references about various features of different models for porous media. Some researchers earlier cited above such as [35-38] have also focused on convective heat transfer with thermal radiation through porous media.

Literature survey reveals that little attention has been paid to the slip flow, heat and mass transfer of non-Newtonian fluids especially Maxwell fluid. Some references earlier cited such as Hayat et al. [3], Sajid et al. [7], and Lin and Guo [29] have examined slip flows of Maxwell fluids under different conditions. Sajid et al. [61] elucidated the fact that fluid patterns characterized by the slip boundary conditions have special significances in many applications. They described that in some instances, the fluids present a loss of adhesion at the wetted wall which compels it to slide along the wall. Consideration for no-slip condition seems unrealistic for many non-Newtonian flows because they exhibit macroscopic wall slip. Particularly, a no-slip condition is inadequate for rough surfaces and in micro electromechanical system (MEMS). The fluid which exhibits boundary slip finds applications in technology such as in the polishing of artificial heart and internal cavities in a variety of manufactured parts are achieved by imbedding such as fluids as abrasive.

In order to fill this gap, the present study focuses on the two dimensional, incompressible and magnetohydrodynamic flow with velocity slip of a non-Newtonian Maxwell fluid over a non-conducting porous stretching surface with a prescribed heat flux considering the fluid to be optically thin. The surface is taken to be permeable in the presence of uniform heat generation/absorption, radiative heat transfer and chemical reaction of order n in a Darcian porous medium. Similarity transformation has been employed for this problem and the dimensionless governing equations are numerically solved. Graphical results for various values of the pertinent parameters are presented to gain a thorough insight into the physics of the

problem. Similarly, the numerical results for local skin friction coefficient, surface temperature and Sherwood number for various values of the embedded parameters are made available in tables in order to gain more insight into the surface shear stress, surface temperature and rate of mass transfer for the problem. To the best of our knowledge, this problem has not been previously studied.

2 Mathematical Analysis

Consider a two-dimensional steady and incompressible boundary layer flow of a non-Newtonian upper-convected Maxwell (UCM) fluid over a non-conducting porous stretching surface with a prescribed heat flux in the presence of thermal radiation and heat source/sink. The fluid under consideration is electrically conducting and optically thin in a Darcian porous medium. The flow which is in the region $y > 0$ is driven by the stretching surface located at $y = 0$. The x axis is chosen along the stretching surface while y - axis is normal to the surface. The prescribed surface heat flux is q_w while the surface species concentration is denoted by C_w. The stretching velocity of the surface is $u_w = m\,x$ with m being a constant. Let the wall constant mass transfer be V_w with $V_w > 0$ for injection and $V_w < 0$ for suction. The flow is presumed to be generated by the stretching surface issuing from a thin slit at the origin. The surface is then stretched in such a way that the speed at any point on the surface becomes proportional to the distance from the origin. The respective free stream temperature and species concentration are T_∞ and C_∞. The flow is subjected to a transverse and uniform magnetic field of strength B_0, which is applied in the positive y - direction, normal to the surface. The induced magnetic field is assumed to be very small in comparison to the applied magnetic field. The chemical reactions are presumed to take place in the flow regime and there exists a homogeneous n^{th} order chemical reaction within the fluid. Following Sadeghy et al. [4] and Hayat and Sajid [62] and based on the aforementioned assumptions, the governing equations of the conservation of mass, momentum, energy and species concentration, using an order magnitude analysis of the y-direction momentum equation (normal to the surface) and the usual boundary layer assumptions with negligible pressure gradient, where other thermophysical properties are kept as constants, can be expressed as follows:

$$\frac{\partial u}{\partial x} + \frac{\partial v}{\partial y} = 0 \tag{1}$$

$$u\frac{\partial u}{\partial x} + v\frac{\partial u}{\partial y} + \lambda\left[v^2\frac{\partial^2 u}{\partial y^2} + 2uv\frac{\partial^2 u}{\partial x \partial y} + u^2\frac{\partial^2 u}{\partial x^2}\right] = \upsilon\frac{\partial^2 u}{\partial y^2} - \frac{\sigma\beta_0^2}{\rho}u - \frac{\upsilon\varphi}{K'}u \tag{2}$$

$$u\frac{\partial T}{\partial x} + v\frac{\partial T}{\partial y} = \omega\frac{\partial^2 T}{\partial y^2} + \frac{1}{\rho Cp}Q\left(T - T_\infty\right) - \frac{1}{\rho Cp}\frac{\partial q_r}{\partial y} \tag{3}$$

$$u\frac{\partial C}{\partial x} + v\frac{\partial C}{\partial y} = D\frac{\partial^2 C}{\partial y^2} - Kr\left(C - C_\infty\right)^n \tag{4}$$

where x, y, u, v, T, C, υ, λ, σ, B_0, ρ, C_p, ω, Q, φ, K', q_r, D, K' and n are coordinate axes along the continuous surface in the direction of motion and normal to it, velocity components in the directions of x and y axes, fluid temperature inside the boundary layer, species concentration of the fluid, kinematic viscosity, relaxation time, electrical conductivity, magnetic field flux, fluid density, specific heat at constant pressure, thermal diffusivity, internal heat generation/absorption,

porosity, permeability of the medium, radiative heat flux, mass diffusivity, rate of chemical reaction and order of chemical reaction respectively.

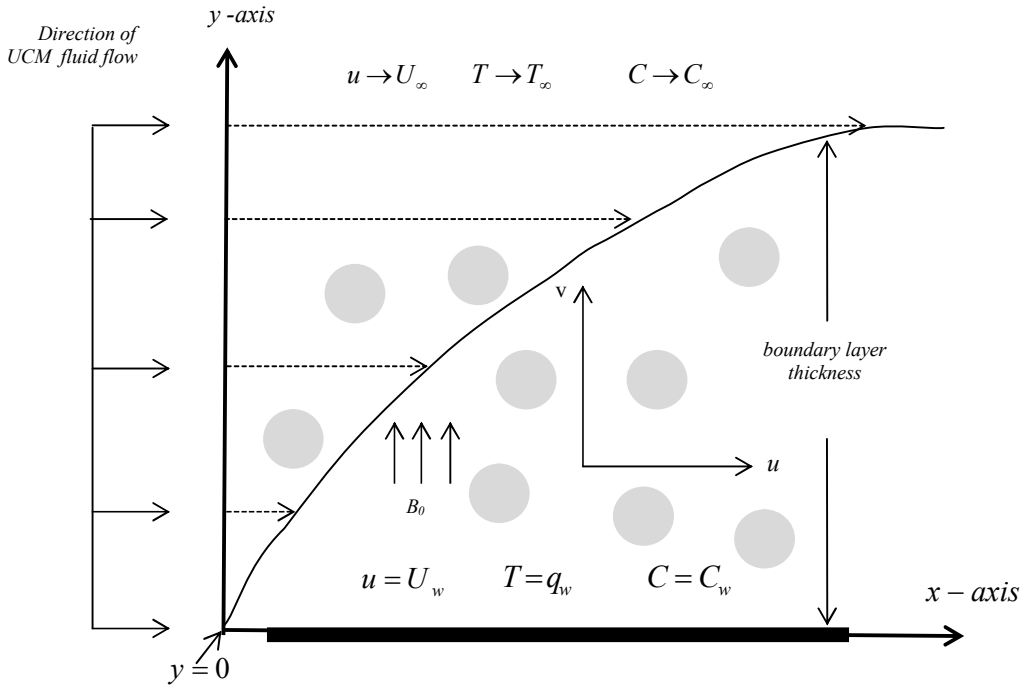

Fig. 1. Sketch of the flow configuration

The boundary conditions for the problem are:

$$u = u_w + E\left(\frac{\partial u}{\partial y}\right), \qquad v = V_w, -\kappa\frac{\partial T}{\partial y} = q_w = Nx^2, \quad C = C_w \quad \text{at } y = 0 \tag{5}$$

$$u \to U_\infty = 0, \qquad T \to T_\infty, \qquad C \to C_\infty \qquad \text{as} \qquad y \to \infty \tag{6}$$

Where κ, q_w, E and N are thermal conductivity, prescribed heat flux, velocity slip factor and a constant respectively. It is worth mentioning that $E = 0$ corresponds to no-slip boundary condition. The above boundary condition is valid when $x << l$ (where l reference length of the surface) which occurs very near to the surface.

Following Cogley et al. [63], it is assumed that the fluid is optically thin with a relatively low density and the radiative heat flux is given by:

$$\frac{\partial q_r}{\partial y} = 4\xi^2\left(T - T_\infty\right) \tag{7}$$

where ξ is the mean radiation absorption coefficient.

Dimensionless quantities are introduced to simplify the mathematical analysis of the problem by introducing the following similarity transformation:

$$\eta = \sqrt{\frac{m}{\upsilon}}y, \qquad \theta(\eta) = \frac{T - T_\infty}{T_w - T_\infty}, \qquad \phi(\eta) = \frac{C - C_\infty}{C_w - C_\infty} \tag{8}$$

The continuity equation (1) is automatically satisfied by chosen a stream function $\psi = \sqrt{m\upsilon}\, x f(\eta)$ as:

$$u = \frac{\partial \psi}{\partial y}, \qquad v = -\frac{\partial \psi}{\partial x} \tag{9}$$

Using the above similarity transformation and equations (5) – (7), the governing equations (2)-(4) are transformed to the following coupled nonlinear ordinary differential equations:

$$f'''(\eta) + f(\eta)f''(\eta) - f'^2(\eta) + \beta\left[2f(\eta)f'(\eta)f''(\eta) - f^2(\eta)f'''(\eta)\right] - (M + Pm)f'(\eta) = 0 \tag{10}$$

$$\theta''(\eta) + \Pr\left[f(\eta)\,\theta'(\eta) - (R - H)\theta(\eta)\right] = 0 \tag{11}$$

$$\phi''(\eta) + \Pr Le\left[f(\eta)\,\phi'(\eta) - \gamma\phi^n(\eta)\right] = 0 \tag{12}$$

with boundary conditions:

$$f(\eta) = s, \qquad f'(\eta) = 1 + \delta f''(\eta), \qquad \theta'(\eta) = -1, \qquad \phi(\eta) = 1 \quad \text{at } \eta = 0 \tag{13}$$

$$f'(\eta) \to 0, \qquad \theta(\eta) \to 0, \qquad \phi(\eta) \to 0 \qquad \text{as } \eta \to \infty \tag{14}$$

where the parameters are defined as:

$\beta = \lambda m$ is the Deborah number, η is the similarity variable, prime is the differentiation with respect to η, f', θ and ϕ are the dimensionless velocity, temperature and species concentration respectively, $Ha = \frac{\sigma\beta_0^2}{m x^2 \rho}$ is the Hartmann number, $\Pr = \frac{\mu C_p}{\kappa}$ is the Prandtl number, $Le = \frac{\omega}{D}$ is the Lewis number, $s = \frac{-V_w}{\sqrt{m\upsilon}}$ is the suction velocity parameter, $Pm = \frac{\upsilon\varphi}{m x^2 K'}$, $\gamma = \frac{Kr}{m}\left(C_w - C_\infty\right)^{n-1}$ is the rate of chemical reaction, $\delta = E\sqrt{\frac{m}{\upsilon}}$ is the velocity slip parameter, $H = \frac{Q}{\rho Cp\, m}$ is the heat source/sink parameter and $R = \frac{4\xi^2 a}{\rho Cp\, m}$ is the thermal radiation parameter.

Other important physical quantities of interest which are germane to the technological and engineering applications of the problem are the local skin friction coefficient C_f, dimensionless surface temperature $\theta(\eta)$ at $\eta = 0$ and Sherwood number Sh_x. The local skin friction coefficient and Sherwood number are respectively defined as:

$$C_f = \frac{\tau_w}{\rho u_w^2} \qquad \Rightarrow \quad C_f\left(\mathrm{Re}_x\right)^{1/2} = \left(1+\beta\right) f''(0) \tag{15}$$

where τ_w is the wall shear stress and Re_x is the local Reynolds number.

$$Sh_x = \frac{x\, h_w}{D\left(C_w - C_\infty\right)} \qquad \Rightarrow \qquad Sh_x\left(\mathrm{Re}_x\right)^{-1/2} = -\phi'(0) \tag{16}$$

where h_w is the mass flux and $\mathrm{Re}_x = \dfrac{xU_w(x)}{\upsilon}$.

3 Computational Procedure

The system of coupled nonlinear ordinary differential equations (10) - (12) with mixed boundary conditions in equations (13) and (14) for different values of emerging parameter, namely: Deborah number β, Hartmann number Ha, Prandtl number Pr, Lewis number Le, velocity slip parameter δ, suction velocity parameter s, Darcian porous medium parameter Pm, heat generation/absorption parameter H, rate of chemical reaction parameter γ, order of chemical reaction parameter n and thermal radiation parameter R has been solved by using an efficient and effective fourth-fifth order Runge-Kutta-Fehlberg (RKF45) method alongside the shooting technique. The nonlinear differential equations (10) – (12) are first decomposed into a system of first order differential equations. The coupled ordinary differential equations (10) - (12) are third order in $f(\eta)$ and second order in $\theta(\eta)$ and $\phi(\eta)$ which have been reduced to a system of seven simultaneous equations for eleven unknowns. To numerically solve this system of equations employing RKF45 method, the solutions require seven initial conditions in all but two initial conditions in $f(\eta)$, one initial condition in each $\theta(\eta)$ and $\phi(\eta)$ are available. However, the values of $f'(\eta), \theta(\eta)$ and $\phi(\eta)$ are known at $\eta \to \infty$. These free stream conditions are used to produce unknown initial conditions at $\eta = 0$ by employing shooting technique. The most important of this algorithm is to choose the appropriate finite value of η_∞. Thus, in order to estimate the value of η_∞, some initial guess values are started with and the boundary value problems consisting of equations (10) - (12) are solved to obtain $f''(0)$, $\theta'(0)$ and $\phi'(0)$. The solution is repeated with another larger value of η_∞ until two successive values of $f''(0), \theta'(0)$ and $\phi'(0)$ differ only after the desired significant digit. The last value η_∞ is taken as the finite value of the limit η_∞ for the particular set of physical parameters for determining the velocity, temperature and the species concentration, which are respectively $f'(\eta), \theta(\eta)$ and $\phi(\eta)$ in the boundary layer. After getting all the initial conditions, this system of simultaneous equations is solved using the RKF45 integration scheme. The value of $\eta_\infty = 10$ has been selected to be appropriate in nearly all cases for the physical parameters governing the flow. Thus, the coupled boundary value problem of third order in $f(\eta)$, second order in $\theta(\eta)$ and $\phi(\eta)$ has been reduced to a system of seven simultaneous equations of the first order for seven unknown variables as follow:

The equations (10) – (12) can be expressed as:

$$f''' = \frac{\left(M + Pm\right) f' + f'^2 - f f'' - 2\beta f f' f''}{\left(1 - \beta f^2\right)} \tag{17}$$

$$\theta'' = -\mathrm{Pr}\left[f\,\theta' - (R - H)\,\theta\right] \tag{18}$$

$$\phi'' = -\Pr Le\left[f\phi' - \gamma\phi^n\right] \tag{19}$$

The following new variables can be defined by the following equations:

$$f_1 = f(\eta)\ , f_2 = f'(\eta), f_3 = f''(\eta),\ f_4 = \theta(\eta),\ f_5 = \theta'(\eta)\ ,\ f_6 = \phi(\eta),\ f_7 = \phi'(\eta) \tag{20}$$

The coupled higher order nonlinear differential equations and the mixed boundary conditions may be transformed to seven equivalent first-order differential equations and the boundary conditions respectively, as follows:

$$\left.\begin{aligned}
f_1' &= f_2 \\
f_2' &= f_3 \\
f_3' &= \frac{(M+Pm)f_2 - f_2^2 - f_1 f_3 - 2\beta f_1 f_2 f_3}{1-\beta f_1^2} \\
f_4^1 &= f_5 \\
f_5^1 &= -\Pr\left[f_1 f_5 - (R-H)f_4\right] \\
f_6^1 &= f_7 \\
f_7^1 &= -\Pr Le\left[f_1 f_7 - \gamma f_6^n\right]
\end{aligned}\right\} \tag{21}$$

Also, the boundary conditions are transformed as:

$$\left.\begin{aligned}
&f_1(0) = s,\ \ f_2(0) = 1 + \delta f_3(0),\quad f_5(0) = -1 \\
&f_6(0) = 1,\ f_2(\infty) = 0,\ f_4(\infty) = 0,\ f_6(\infty) = 0
\end{aligned}\right\} \tag{22}$$

Hence, the boundary value problem in equations (10) – (12) with the boundary conditions (13) and (14) is now converted into an initial value problem in equation (21) with the initial conditions in equation (22). Then, the initial value problem is solved by employing RKF45 integrating scheme and by appropriately guessing the missing initial values using the shooting method. For several sets of pertinent parameters, the step size of $\Delta\eta = 0.001$ is used for the computational purposes by translating the algorithm into MAPLE code as described by Heck [64] and error tolerance of 10^{-7} is used in all the cases. The results obtained are presented through graphs for velocity, temperature and species concentration profiles and through tables for local skin-friction coefficient, surface temperature and Sherwood number.

4 Results and Discussion

Numerical solutions are obtained for the velocity, temperature and species concentration fields for different values of governing parameters. Results are displayed through graphs in Figs. 2-19. It should be noted that Figs. 2-7 satisfy the specified boundary conditions and Figs. 8-19 reveal that the far field boundary conditions are satisfied asymptotically and hence this supports the accuracy of the numerical computations and results. Moreover, the behaviour of skin friction coefficient, dimensionless surface temperature and Sherwood number due to the variations in various emerging parameters is also deliberated in Tables 1 and 2.

4.1 Velocity profiles

The velocity profiles f' for different values of Deborah number β, Hartmann number Ha, thermal radiation parameter R, velocity slip parameter δ, Darcian porous medium parameter Pm and suction parameter s are displayed in Figs. 2-7 respectively. Fig. 2 shows the influence of β on the flow distribution. It is evident from this figure that f' is a decreasing function of β. This implies that a decrease in the fluid velocity corresponds to an enhancement of the velocity boundary layer thickness. From the physical point of view, when shear stress is eliminated, the fluid will come to rest. This kind of phenomenon is experienced in many polymeric liquids that cannot be defined in the viscous fluid model. Higher values of β will produce a retarding force between two adjacent layers in the flow. For this reason, there will be a reduction in the velocity profile and corresponding associated effect is noticed in the boundary layer thickness. Fig. 3 depicts the effect Ha on f'. It is obvious that an increase in the values of Ha decrease the boundary layer thickness in the flow distribution. Hartmann number refers to the ratio of electromagnetic force to the viscous force. This implies that the electromagnetic force controls the flow distribution and this leads to an increase in the velocity profile. Fig. 4 illustrates the influence of thermal radiation parameter R on f'. An increase in the values of R is observed to reduce the velocity profile. The effect of velocity slip parameter δ on f' is depicted in Fig. 5. f' is found to be an increasing function of δ. This is anticipated as there is a critical shear rate of the polymeric Maxwell fluid initiated by the stretching surface. The bound polymers begin to detach from the stretched surface polymers, resulting in the relative sliding of bulk and surface layers. The sliding velocity in the flow regime increases with increasing shear rate. Hence, an increment in δ corresponds to an increasing velocity profile. Fig. 6 displays the effect of Pm on the velocity profile. An increase in the values of Pm decreases the velocity profile. On observing Fig. 7, as the values of s increase, the velocity profile decreases as anticipated. This implies that suction which is the removal of fluid from the domain via the porous surface can be used to exercise controls over the fluid dynamics. Thus, suction enhances adherence of the fluid to the surface which in turn retards the flow.

4.2 Temperature profiles

Figs. 8 - 12 illustrate the variations of θ with respect to η for various values of Ha, R, s, $\Pr$ and H respectively. From Fig. 8, it is observed that Ha has a decreasing effect on θ. A higher value of Ha corresponds to a higher value of an electromagnetic force in comparison to a viscous force. Thus, a decrease in the fluid temperature in the flow distribution with its consequent reduction in the thermal boundary layer thickness is noticeable when the values of Ha increase. The influence of thermal radiation R on θ is portrayed by Fig. 9. The thermal boundary layer thickness decreases as the values of R increase. Fig. 10 expresses the effect of s on the temperature profile. Suction velocity parameter is also found to reduce the fluid temperature. The feature of $\Pr$ on θ is displayed in Fig. 11. $\Pr$ is a decreasing function of the temperature profile. Higher estimation of $\Pr$ is found to decay the temperature distribution in the flow regime. This is due to the fact that $\Pr$ expresses the ratio of thermal diffusivity to momentum diffusivity. Thus, small values of $\Pr$ implies that the thermal diffusivity dominates and for higher estimation of $\Pr$, the momentum diffusivity dominates. As the values of H increase, the temperature profile increases for both cases of heat generation and heat absorption as shown in Fig. 12. Positive values of H corresponds to heat generation whereas negative values of H signifies heat absorption. Though, when heat generation is considered in the flow regime, the fluid temperature is higher than that of heat absorption. Consequently, the thermal boundary layer thickness and the surface temperature are enhanced by increment in the values of H.

4.3 Species concentration profiles

Figs. 13 - 19 describe the influences of Ha, R, γ, s, $\Pr$, Le and n on the species concentration profile. Fig. 13 captures the influence of Ha on the species concentration profile. It is observed that for any

given value of η, the species concentration becomes decreased with an increase in Ha. The variation of ϕ with different values of R is indicated by Fig. 14. It is clear that the thermal radiation parameter decreases the species concentration profile. Fig. 15 is plotted to display the influence of γ on species concentration distribution in the boundary layer. It is observed that increasing the values of γ corresponds to a decrease in the species concentration boundary layer thickness. In Fig. 16, it is interesting to note that s is a decreasing function of the species concentration boundary layer. This establishes the facts that suction velocity parameter can be employed to control the fluid species concentration in the flow regime. In Figs. 17 and 18, it is interesting to note that $\Pr$ and Le have the same effects on the species concentration boundary layer. Both of them noticeably decrease the concentration layer thicknesses. Lewis number which is the ratio of thermal diffusivity to mass diffusivity is used to characterize fluid flows where there is simultaneous heat and mass transfer. The implication of the reduction in the fluid species concentration is that the thermal diffusivity has more influence over both momentum and mass diffusivities in the flow regime. Lastly, Fig. 19 is plotted to display the influence of n on the species concentration profile. The species concentration boundary layer thickness is found to increase with increment in the values of the order of chemical reaction parameter.

Tables 1 and 2 present variations of local skin friction coefficient, dimensionless surface temperature and Sherwood number in relation to β, Ha, s, Pm, R, $\Pr$, Le, δ, H, γ and n. These tables show that as the values of Hartmann number, Darcian porous medium, velocity slip parameter, heat absorption parameter and rate of chemical reaction parameter increase, the values of local skin friction coefficient increase. However, the skin friction coefficient is found to decrease as the values of Deborah number, suction velocity parameter, thermal radiation parameter, Prandtl number, Lewis number, heat generation parameter and order of chemical reaction parameter increase. Also, it is worthy to note that as the values of β, H and n increase, the dimensionless surface temperature increases whereas an increase in the values of Ha, s, Pm, R, $\Pr$, Le, δ and γ are found to decrease the dimensionless surface temperature. Finally, it is evident from these tables that the local rate of mass transfer is enhanced by increasing the values of Hartmann number, suction velocity, Darcian porous medium, velocity slip, heat absorption and rate of chemical reaction parameters. However, as the values of Deborah number, Prandtl number, Lewis number, heat generation and order of chemical reaction increase, the local Sherwood number decreases.

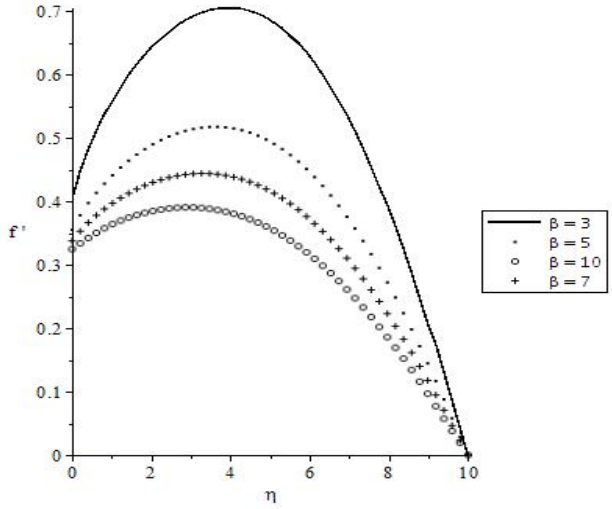

Fig. 2. Variation of β on velocity profile for $Ha = 0.5$, $Pm = 3$, $s = 0.5$, $\delta = 0.5$

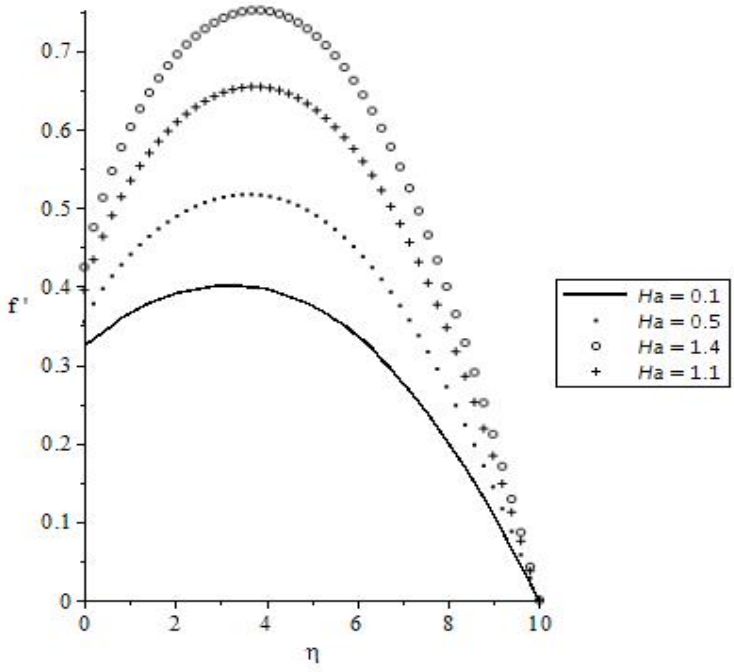

Fig. 3. Variation of Ha on velocity profile for $\beta = 0.01,\ Pm = 3,\ s = 0.5,\ \delta = 0.5$

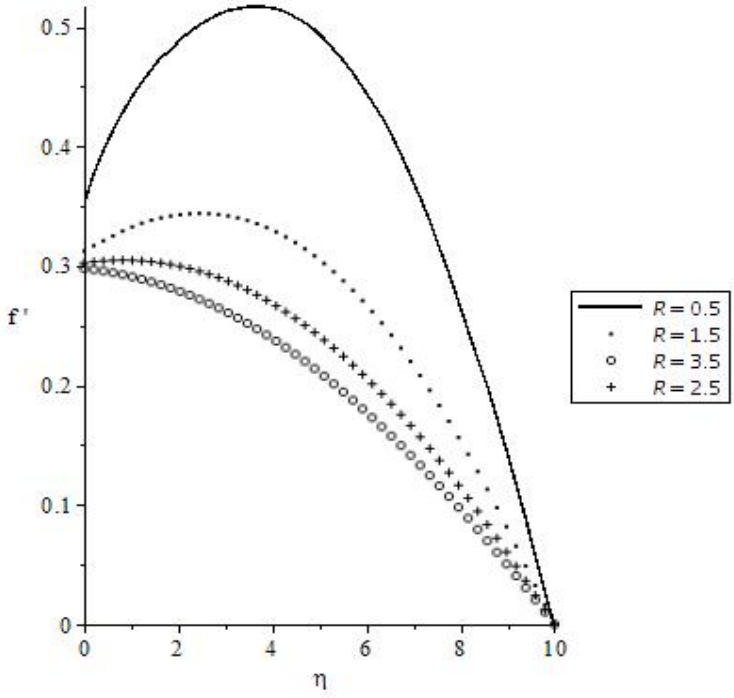

Fig. 4. Variation of R on velocity profile for $\beta = 0.01,\ Ha = 0.5,\ Pm = 3,\ s = 0.5,\ \delta = 0.5$

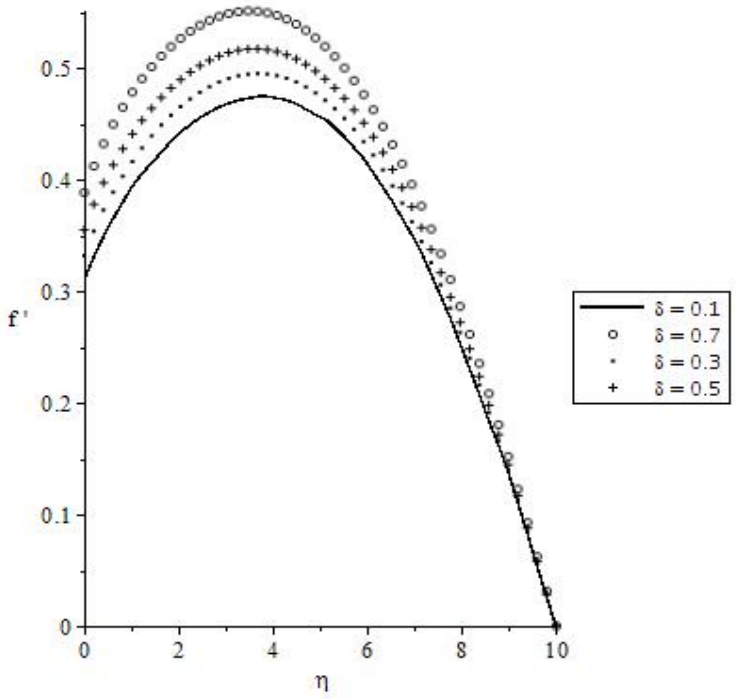

Fig. 5. Variation of δ on velocity profile for $\beta = 0.01,\ Ha = 0.5,\ Pm = 3,\ s = 0.5$

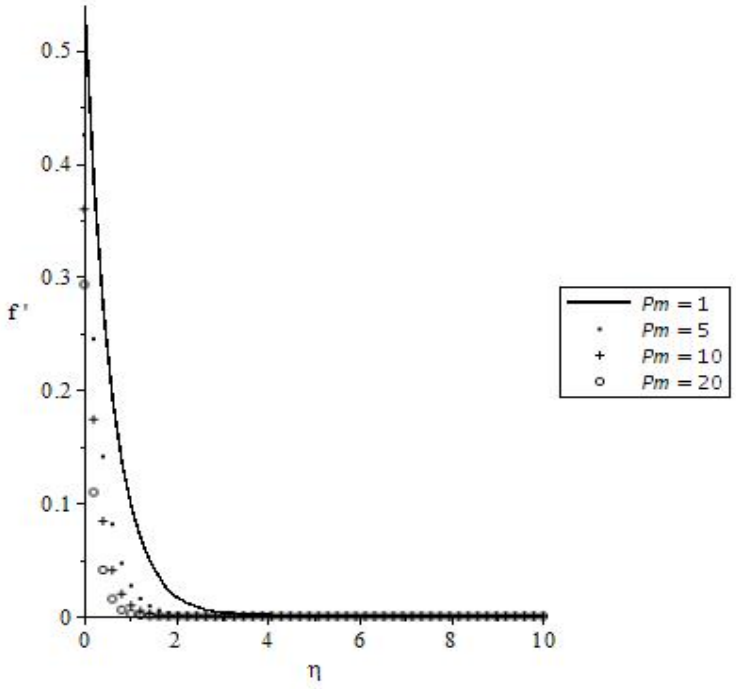

Fig. 6. Variation of Pm on velocity profile for $\beta = 0.01,\ Ha = 0.5,\ s = 0.5,\ \delta = 0.5$

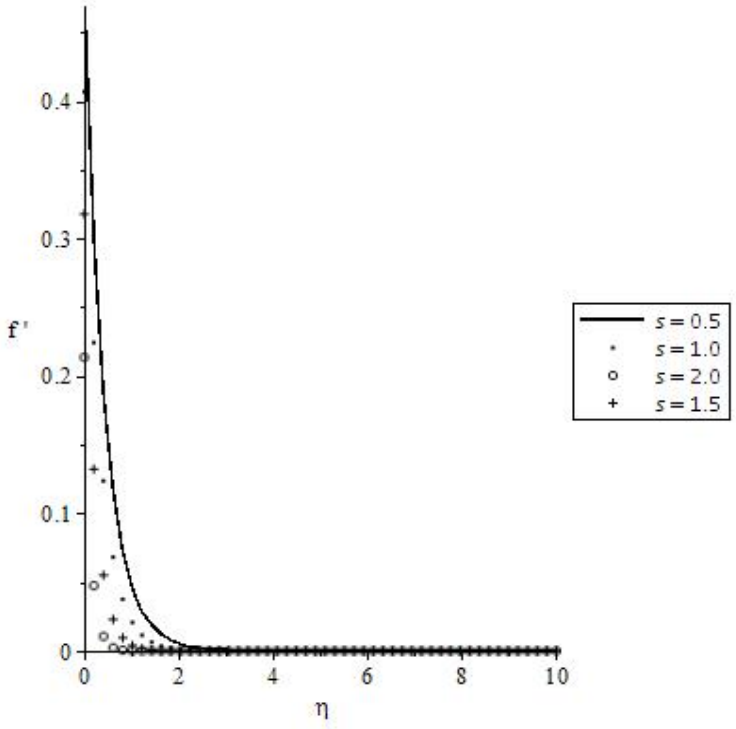

Fig. 7. Variation of s on velocity profile for $\beta = 0.01,\ Ha = 0.5,\ Pm = 3,\ \delta = 0.5$

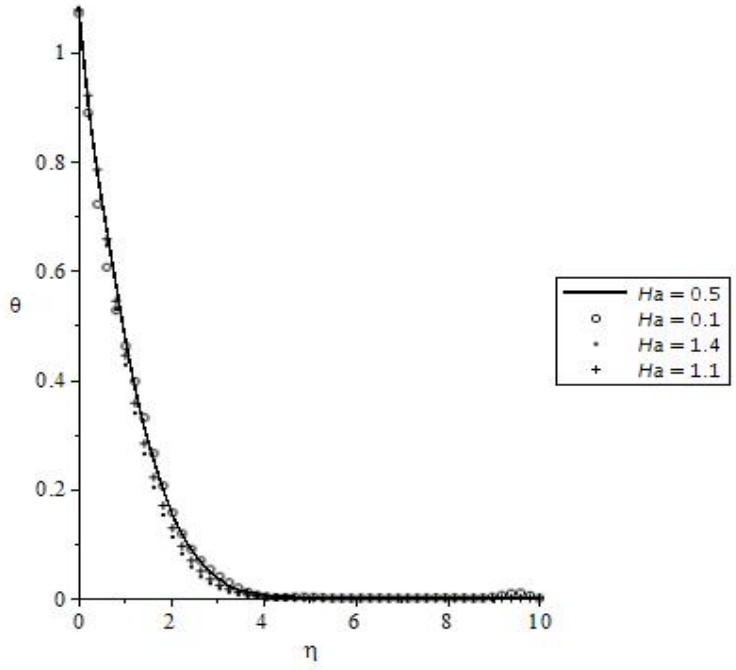

Fig. 8. Variation of Ha on temperature profile for $\beta = 0.01,\ \Pr = 0.71,\ R = 2,\ s = 0.5,\ H = 1$

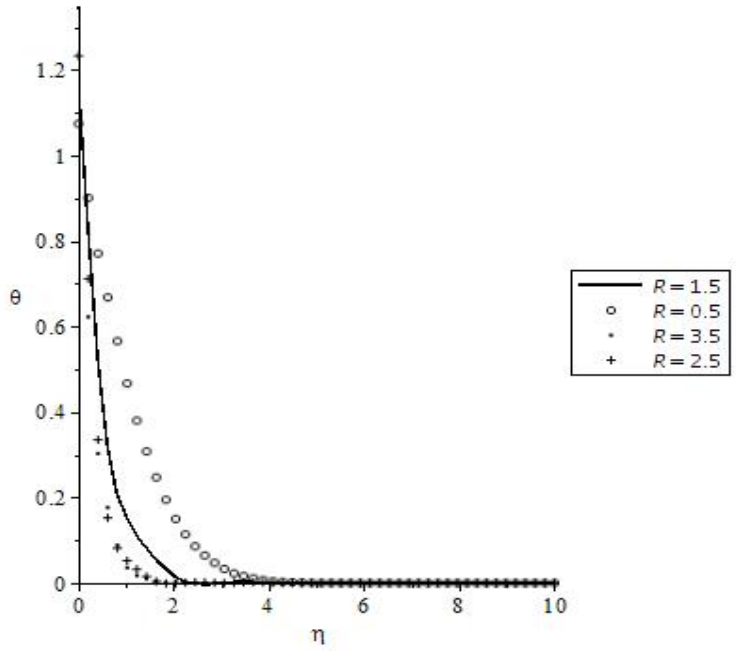

Fig. 9. Variation of R on temperature profile for $\beta = 0.01,\ \Pr = 0.71,\ s = 0.5,\ H = 1$

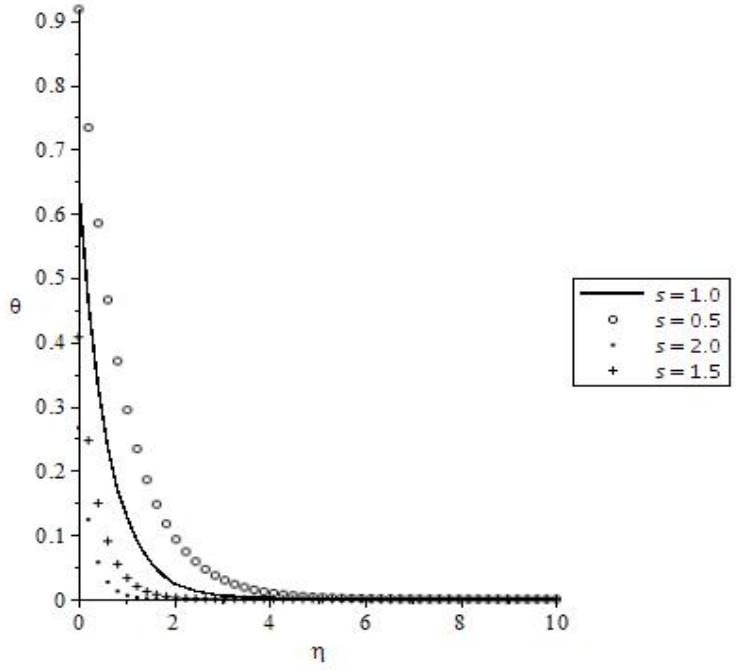

Fig. 10. Variation of s on temperature profile for $\beta = 0.01,\ \Pr = 0.71,\ R = 2,\ H = 1$

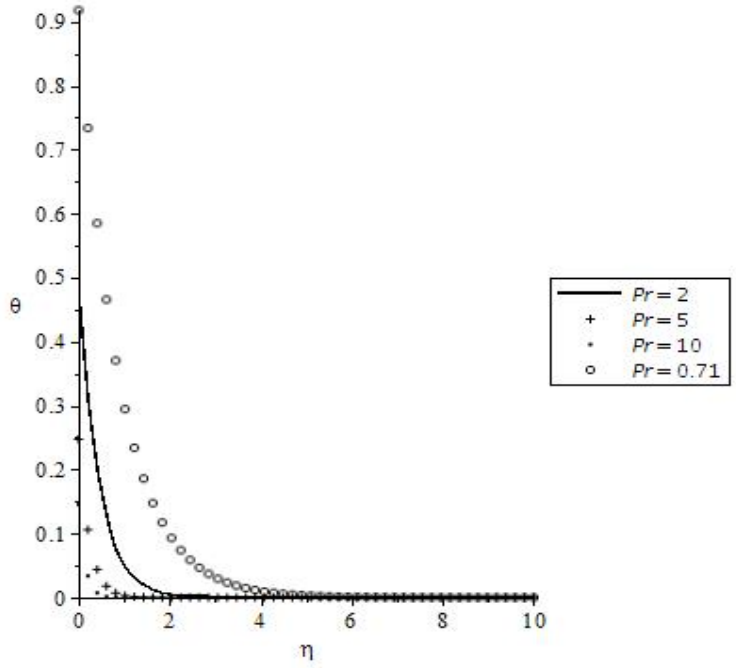

Fig. 11. Variation of $\Pr$ **on temperature profile for** $\beta = 0.01,\ R = 2,\ s = 0.5,\ H = 1$

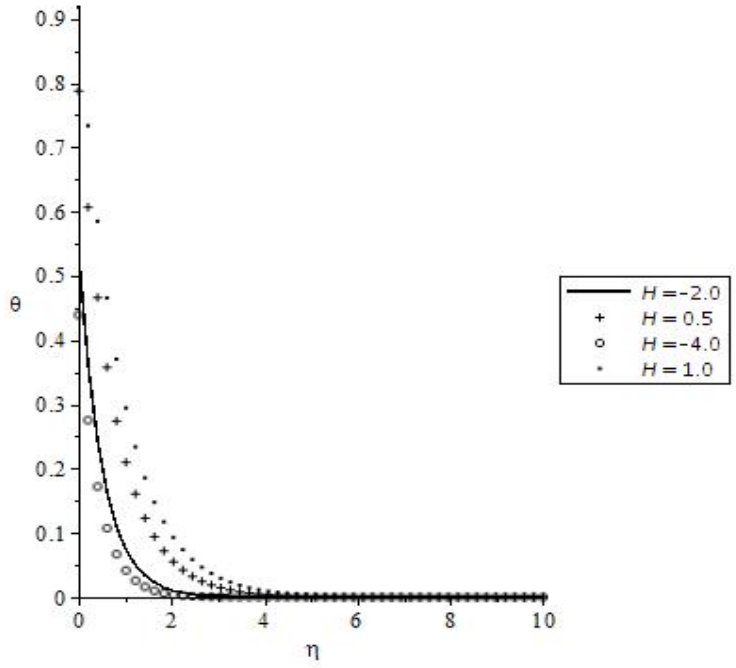

Fig. 12. Variation of H **on temperature profile for** $\beta = 0.01,\ \Pr = 0.71,\ R = 2,\ s = 0.5$

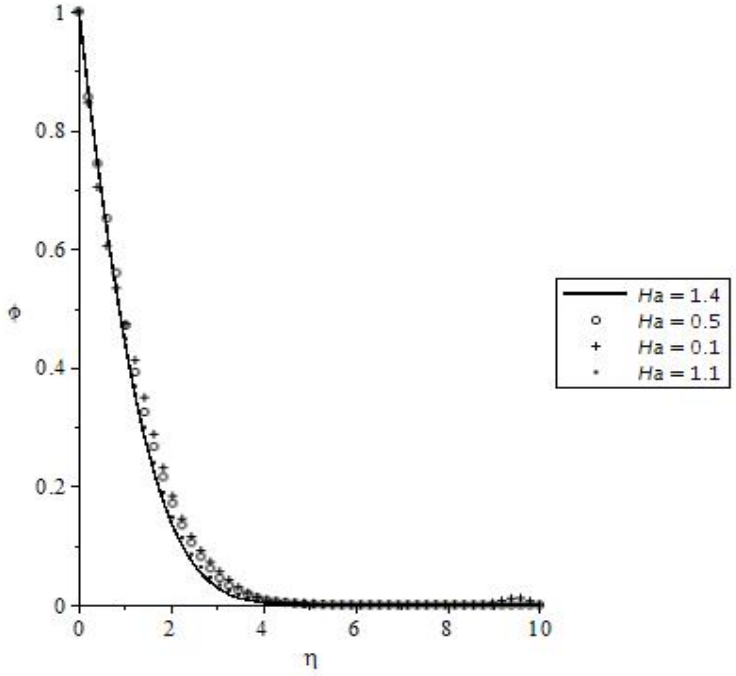

Fig. 13. Variation of Ha on concentration profile for $\gamma = 1$, $\Pr = 0.71$, $Le = 1.32394$

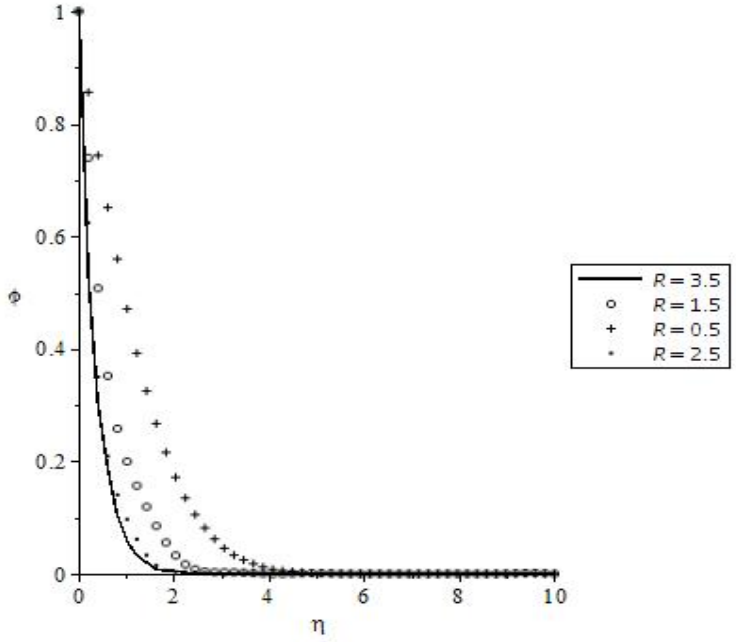

Fig. 14. Variation of R on species concentration profile for $\gamma = 1$, $\Pr = 0.71$, $Le = 1.32394$

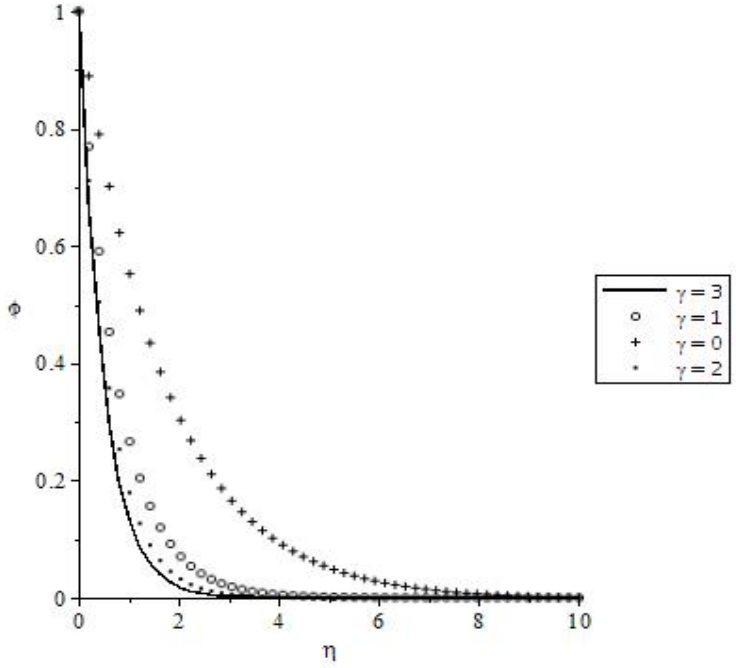

Fig. 15. Variation of γ on species concentration profile for $s = 0.5,\ \mathrm{Pr} = 0.71,\ Le = 1.32394$

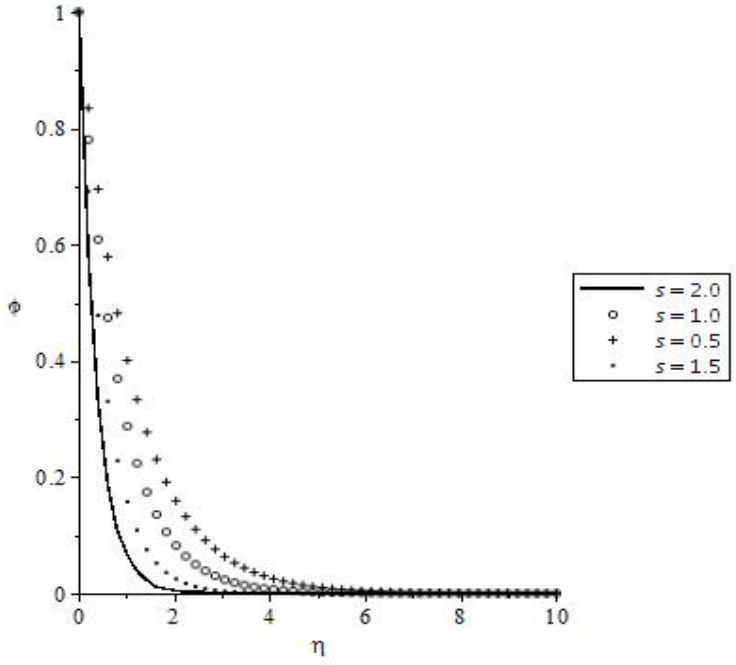

Fig. 16. Variation of s on species concentration profile for $\gamma = 1,\ \mathrm{Pr} = 0.71,\ Le = 1.32394$

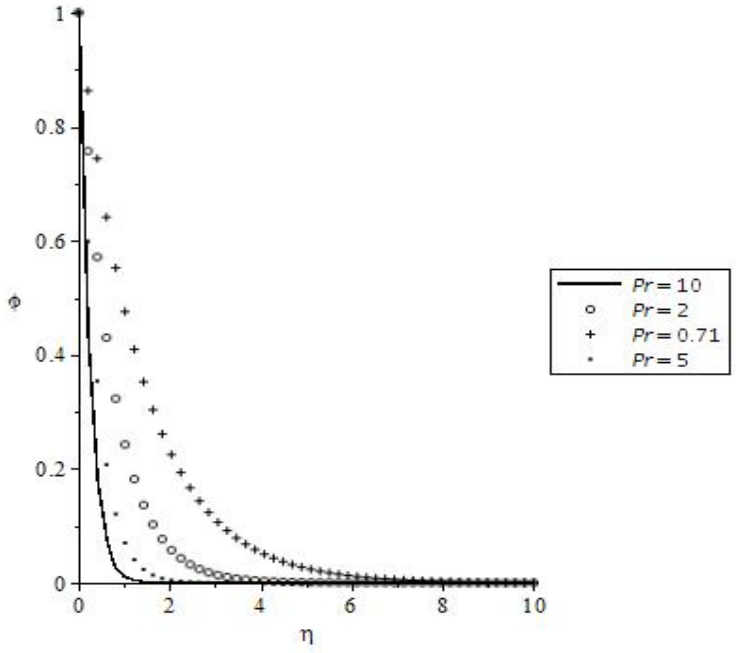

Fig. 17. Variation of $\Pr$ **on species concentration profile for** $\gamma = 1,\ s = 0.5,\ Le = 1.32394$

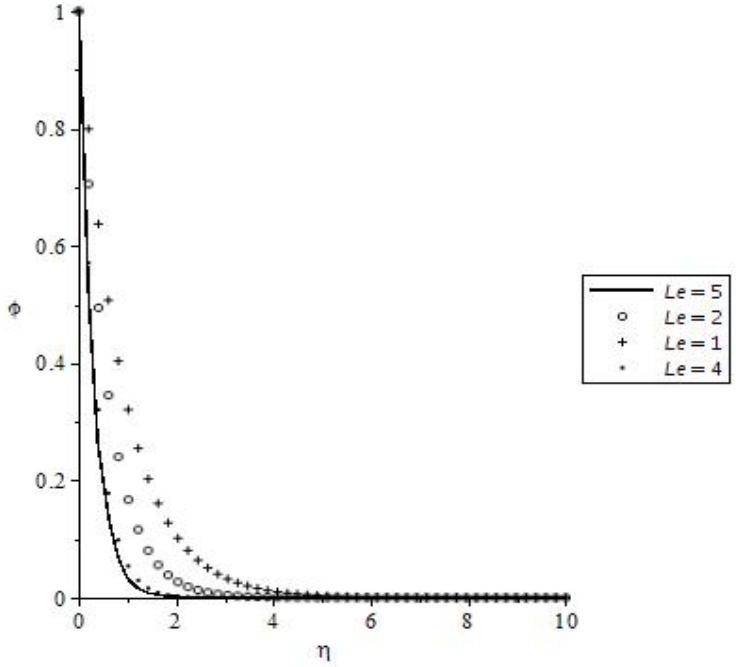

Fig. 18. Variation of Le **on species concentration profile for** $\gamma = 1,\ \Pr = 0.71,\ s = 0.5$

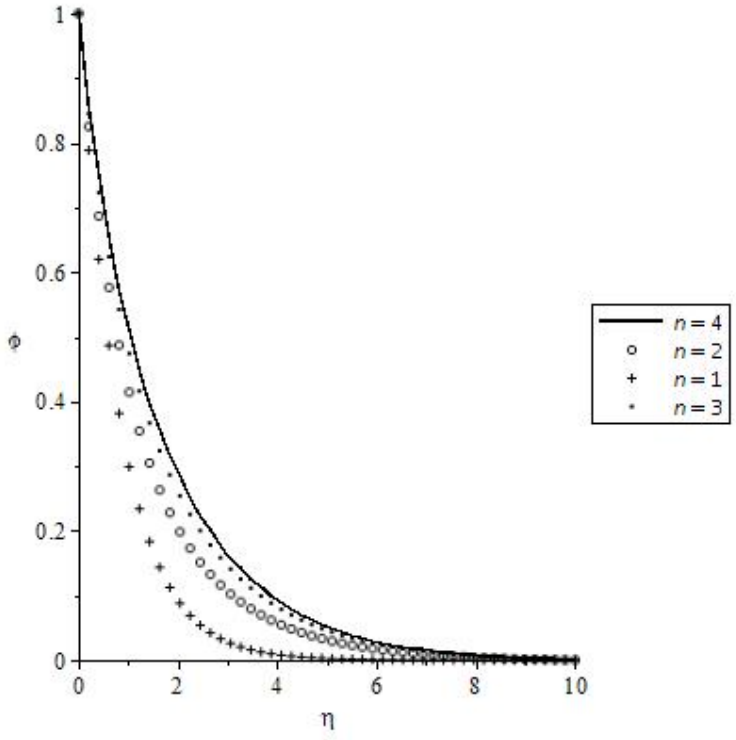

Fig. 19. Variation of n on species concentration profile for $s = 0.5$, $\Pr = 0.71$, $Le = 1.32394$

Table 1. Values of local skin friction coefficient, surface temperature and Sherwood number when $\beta = 10$, $s = 0.5$, $Ha = 5$, $Pm = 3$, $R = 2$, $\delta = 0.5$, $Le = 1.32394$, $\Pr = 0.71$, $\gamma = 1$

β	Ha	s	Pm	R	$f''(0)$	$\theta(0)$	$-\phi'(0)$
10					0.670143421437399	0.730079179768046	1.61305817472367
20					0.314910000774969	0.757470131959812	1.55727112308650
30					0.205941506976925	0.766956465924263	1.53896768485879
	5				0.670143421437399	0.730079179768046	1.61305817472367
	10				1.045308910129090	0.705201303081446	1.66770762427392
	15				1.421493202664490	0.683463911626964	1.71888531810080
		1.5			0.195013066763355	0.555339748399596	2.21055955126873
		2.0			0.140148653285598	0.484092152598781	2.57318131895424
		3.0			0.081209677691928	0.378473117591700	3.35869839065528
			5		0.820059545792069	0.719693201759715	1.63538767870157
			8		1.045308910129090	0.705201303081446	1.66770762427392
			12		1.346192059840010	0.687597689227729	1.70889272552484
				1	0.670143421431766	0.941898776276787	1.61305817472310
				3	0.670143421352667	0.615784802124303	1.61305817471516
				5	0.670143421162864	0.490109007189548	1.61305817469608

Table 2. Values of local skin friction coefficient, surface temperature and Sherwood number when $\beta = 10,\ s = 0.5,\ Ha = 5,\ Pm = 3,\ R = 2,\delta = 0.5,\ Le = 1.32394,\ \Pr = 0.71,\ \gamma = 1$

Pr	Le	δ	H	γ	n	$f''(0)$	$\theta(0)$	$-\phi'(0)$
1						0.670143421321513	0.597704147841781	1.61305817471203
1.8						0.670143421013099	0.418444903913972	1.61305817468103
2.5						0.670143420769971	0.339944094031206	1.61305817465660
	1.00					0.670143421895727	0.730079179746992	1.36971444706406
	1.10					0.670143421492662	0.730079179765515	1.44739657401267
	1.39					0.670143421159202	0.730079179780830	1.66007034154426
		0.1				0.647851943611487	0.758869943021600	1.55266976727577
		0.4				0.664520848545271	0.737157013177289	1.59778870453003
		0.8				0.687292558214682	0.709332057355312	1.65952602103773
			-4			0.670143420993856	0.419488014617078	1.61305817467910
			-2			0.670143421162864	0.490109007189548	1.61305817469608
			1			0.670143421437399	0.730079179768046	1.61305817472367
			2			0.670143421431766	0.941898776276787	1.61305817472310
				2		0.670143421371819	0.730079179771046	1.90439938376314
				3		0.670143421419625	0.730079179768838	2.15690267895844
				4		0.670143421567713	0.730079179762021	2.38225825618070
					0	0.670143421862403	0.730079179748426	3.45089816953900
					1	0.670143421437399	0.730079179768046	1.61305817472367
					2	0.670143421284530	0.730079179775080	1.49189486776958

5 Conclusions

The present study proposes a numerical approach of RKF45 with shooting technique to solve the heat and mass transfer of a MHD reactive flow of an upper-convected Maxwell fluid model over a stretching surface subjected to a prescribed heat flux with velocity slip effect in a Darcian porous medium in the presence of thermal radiation, internal heat generation/absorption and chemical reaction of order n. The accuracy of the numerical computations and results is supported by the velocity profiles satisfying the specified boundary conditions while both temperature and species concentration profiles establish that the far field boundary conditions are asymptotically satisfied. The results of physical interests on the velocity, temperature and species concentration profiles as well as the wall shear stress, surface temperature and rate of mass transfer at the wall are summarized below:

1. The velocity distribution increases for higher estimation of velocity slip parameter and Hartmann number but it decays with increasing values of Deborah number, thermal radiation parameter, Darcian porous medium parameter and suction velocity parameter;
2. The temperature distribution is enhanced by increasing values of both heat generation and heat absorption parameters. However, the temperature is a decreasing function of thermal radiation parameter, Prandtl number, Hartmann number and suction velocity parameter;
3. The species concentration distribution increases by increasing values of order of chemical reaction parameter whereas the species concentration is found to decay with increment in the values of thermal radiation parameter, Hartmann number, Lewis number, Prandtl number, suction velocity parameter and rate of chemical reaction parameter;
4. Increasing values of Hartmann number, Darcian porous medium and velocity slip parameters have boosting effects on the local skin friction coefficient and local rate of mass transfer whereas these parameters are found to decrease the fluid temperature at the stretching surface.

Competing Interests

Authors have declared that no competing interests exist.

References

[1] Fetecau C, Fetecau C. A new solution for the flow of a Maxwell past an insulated plate. International Journal of Non-Linear Mechanics. 2003;38:423-427.

[2] Abbas Z, Sajid M, Hayat T. MHD boundary layer flow of an upper-convected Maxwell fluid in porous channel. Theoretical Computational Fluid Dynamics. 2006;20:229–238.

[3] Hayat T, Hina S, Hendi AA. Slip effects on the magnetohydrodynamic peristaltic flow of a Maxwell fluid, Z. Naturforsh. 2010;65:1123-1136.

[4] Sadeghy K, Najafi AH, Saffaripour M. Sakiadis flow of an upper-convected Maxwell fluid. International Journal of Non-Linear Mechanics. 2005;40:1220-1228.

[5] Zierep J, Fetecau C. Energetic balance for the rayleigh-stokes problem of a Maxwell fluid. International Journal of Engineering Science. 2007;45(2):617-627.

[6] Wang SW, Tan WC. Stability analysis of double-diffusive convection of Maxwell fluid in a porous medium heated from below. Physics Letter A. 2008;372:3046-3050.

[7] Sajid M, Abbas Z, Ali N, Javed T, Ahmad I. Slip flow of a Maxwell fluid past a stretching sheet. Walailak Journal of Science and Technology. 2014;11(12):1093-1103.

[8] Shateyi S, Motsa SS, Makukula Z. On spectral relaxation method for entropy generation in a MHD flow and heat transfer of a Maxwell fluid. Journal of Applied Fluid Mechanics. 2015;8 (1):21-31.

[9] Adegbie KS, Omowaye AJ, Disu AB, Animasaun IL. Heat and mass transfer of upper convected Maxwell fluid flow with variable thermophysical properties over a horizontal melting surface. Applied Mathematics. 2015;6(08): 8410.
DOI: 10.4236/am.2015.68129

[10] Omowaye AJ, Animasaun IK. Upper-convected Maxwell fluid flow in variable thermophysical properties over a melting surface situated in hot environment subject to thermal stratification. Journal of Applied Fluid Mechanics. 2016;9(4):1777-1790.

[11] Koríko OK, Adegbie KS, Omowaye AJ, Animasaun IL. The boundary layer of an Upper- convected Maxwell fluid flow with variable thermo-physical properties over a melting thermally stratified surface. FUTA Journal of Research in Sciences. 2016;12(2):287-298.

[12] Rahbari A, Abbasi M, Rahimipetroudi I, Sundén B, Domiri GD, Gholami M. Heat transfer and MHD flow of non-Newtonian Maxwell fluid through a parallel plate channel: Analytical and numerical solution. Mechanical Sciences. 2018;9:61-70.
Available: https://doi.org/10.5194/ms-9-61-2018

[13] Khan H, Haneef M, Shah Z, Islam S, Khan W, Muhammad S. The combined magnetohydrodynamic and electric field effect on an unsteady Maxwell nanofluid Flow over a Stretching Surface under the Influence of Variable Heat and Thermal Radiation. Appl. Sci. 2018;8:160.
DOI: 10.3390/app8020160

[14] Hayat T, Sajid M. Serial solution for the upper-convected Maxwell fluid over a porous stretching plate. Physics Letters A. 2006;358:396-403.

[15] Hayat T, Abbas Z. Ali N. MHD flow and mass transfer of an upper-convected Maxwell fluid past a porous shrinking sheet with chemical reaction species. Physics Letters A. 2008;372(26):4698-4704. DOI: 10.1016/j.physleta.2008.05.006

[16] Ishak N, Hashim H, Mohamed MKA, Sarif NM, Khaled M, Rosli N, Salleh MZ. MHD flow and heat transfer for the upper-convected Maxwell fluid over a stretching/shrinking sheet with prescribed heat flux. AIP Conference Proceedings. 2015;1691:040011.
Available: https://doi.org/10.1063/1.4937061

[17] Mustafa M, Khan JA, Hayat T, Alsaedi A. Simulations for Maxwell fluid flow past a convectively heated exponentially stretching sheet with nanoparticles. AIP Advances. 2015;5:037133.
Available: https://doi.org/10.1063/1.4916364

[18] Hayat T, Ashraf BM, Alsaedi A, Shehzad SA. Convective heat and mass transfer effects in three-dimensional flow of Maxwell fluid over a stretching surface with heat source. Journal of Central South University. 2015;22(2):717-726.

[19] Mushtaq A, Mustafa M, Hayat T, Alsaedi A. Effects of thermal radiation on the stagnation-point flow of upper-convected Maxwell fluid over a stretching sheet. Journal of Aerospace Engineering. 2014;27(4): 04014015.
DOI: 10.1061/(ASCE)AS.1943-5525.0000361

[20] Pop I, Sujatha A, Vajravelu K, Prasad KV. MHD Flow and Heat Transfer of a UCM Fluid over a Stretching Surface with Variable Thermophysical Properties. Meccanica. 2012;47:1425-1439.
Available: http://dx.doi.org/10.1007/s11012-011-9526-x

[21] Hayat T, Abbas Z, Sajid M. Series solution for the upper-convected Maxwell fluid over a porous stretching plate. Physics Letter A. 2006;358:396-403.

[22] Shah Z. Islam S, Gul Z, Bonyah E, Khan MA. The electrical MHD and hall current impact on micropolar nanofluid flow between rotating parallel plates. Results in Physics. 2018;9:1201-1214. DOI: doi.org/10.1016/j.rinp.2018.01.064

[23] Shah Z, Gul T, Khan AM, Ali I, Islam S, Hussain F. Effects of hall current on steady three dimensional non-Newtonian nanofluid in a rotating frame with brownian motion and thermophoresis effects. Journal of Engineering Technology. 2018;6:280-296.

[24] Khater AH, Callebaut DK, Malfliet W, Seadawy AR. Nonlinear dispersive Rayleigh-Taylor instabilities in magnetohydro-dynamic flows, Physica Scripta. 2001;64:533-547.
DOI: 10.1238/Physica.Regular.064a00533

[25] Hayat T, Abbas Z, Ali N. MHD flow and mass transfer of an upper-convected Maxwell fluid past a porous shrinking sheet with chemical reaction species. Physics Letters A. 2008;372(26):4698-4704. DOI: 10.1016/j.physleta.2008.05.006

[26] Baoku IG, Olajuwon BI, Mustapha AO. Heat and mass transfer on a MHD third -grade fluid with partial slip flow past an infinite vertical insulated porous plate in a porous medium. International Journal of Heat and Fluid Flow. 2013;40:81 – 88.

[27] Olajuwon BI, Baoku IG, Agboola AAA. Numerical study of a hydromagnetic partial slip flow, heat and mass transfer of a third grade fluid with the presence of thermal radiation through a porous medium. International Journal of Energy and Technology (IJET). 2014;6(19):1-17.

[28] Shateyi S, Motsa SS, Makukula Z. On spectral relaxation method for entropy generation in a MHD flow and heat transfer of a Maxwell fluid. Journal of Applied Fluid Mechanics. 2015;8(1):21-31.

[29] Lin Y. Guo B. Effect of second-order slip on the flow a fractional Maxwell MHD fluid. Journal of the Association of Arab Universities for Basic and Applied Sciences. 2017;24:232-241.

[30] Gaffar S, Prasad VR, Beg OA, Khan HH, Venkatadri K. Radiative and magnetohydrodynamic flow of third-grade viscoelastic fluid past an isothermal inverted cone in the presence of heat generation/absorption. Journal of the Brazilian Society of Mechanical Sciences and Engineering. 2018;40:127.
DOI: org/10.1007/s40430-018-1049-0

[31] Eckert ERG, Drake RM. Heat and Mass Transfer, Second ed. Tata McGraw-Hill, New Delhi; 1979.

[32] Gorla RSR. Radiative effect on conjugate forced convection and conductive heat transfer in a circular pin. International Journal of Heat and Fluid Flow. 1988;9:49–51.

[33] Raptis A, Massalas CV. Magnetohydrodynamic flow past a plate by the presence of radiation. Heat and Mass Transfer. 1998;34:107-109.

[34] Pop SR, Grosan T, Pop I. Radiation effects on the flow near a stagnation point of a stretching sheet. Tech. Mech. 2004;25:100-106.

[35] Abdul Hakeem AK, Sathiyanathan K. An analytic solution of an oscillatory flow through a porous medium with radiation effect. Nonlinear Analysis: Hybrid Systems. 2009;3:288-295.

[36] Hossain MA, Alim MA, Rees DAS. The effect of radiation on free convection from a porous vertical plate, Int. J. Heat Mass Transfer. 1999;42:181–191.

[37] Hayat T, Abbas Z, Pop I, Asghar S. Effects of radiation and magnetic field on the mixed convection stagnation-point flow over a vertical stretching sheet in a porous medium. International Journal of Heat and Mass Transfer. 1999;53:466-474.

[38] Baoku IG, Israel-Cookey C, Olajuwon BI. Influence of thermal radiation on a transient MHD couette flow through a porous medium. Journal of Applied Fluid Mechanics. 2012;5(1):81 – 87.

[39] Gorla RSR. Pop I. Conjugate heat transfer with radiation from a vertical circular pin in non-Newtonian ambient medium. Warme Stoffubertr. 1993;28:11-15.

[40] Siddheshwar PG, Mahabaleshwar US. Effect of radiation and heat transfer on MHD flow of viscoelastic liquid and heat transfer over stretching sheet. International Journal of Nonlinear Mechanics. 2005;40:807-820.

[41] Olajuwon BI, Baoku IG. Numerical study of heat and mass transfer in a transient third grade fluid flow in the presence of heat source, chemical reaction and thermal radiation. Daffodil International University Journal of Science and Technology. 2014;9(2):25-36.

[42] Aliakbar V, Alizadeh-Pahlavan A, Sadeghy K. The influence of thermal radiation on MHD flow of Maxwellian fluids above stretching sheets, Communication in Nonlinear Science and Numerical Simulation. 2009;14:779-794.

[43] Mushtaq A, Mustafa M, Hayat T, Alsaedi A. Effects of thermal radiation on the stagnation-point flow of upper-convected Maxwell fluid over a stretching sheet. Journal of Aerospace Engineering. 2014;27(4):04014015.
DOI: 10.1061/(ASCE)AS.1943-5525.0000361

[44] Bilal M, Sagheer M, Hussain S. On MHD 3D upper convected Maxwell fluid flow with thermophoretic effect using nonlinear radiative heat flux. Canadian Journal of Physics. 2018;96(1):1-10.

[45] Baoku IG, Fadare SA. Thermo-diffusion and diffusion-thermo effects on mixed convection hydromagnetic flow in a third grade fluid over a stretching surface in a Darcy-Forchheimer porous medium, FUDMA Journal of Science. 2018;2(1):23-42.

[46] Shah Z, Islam S, Ayaz H, Khan S. Radiative heat and mass transfer analysis of micropolar nanofluid flow of Casson fluid between two rotating parallel plates with effects of Hall current. ASME Journal of Heat Transfer; 2018.
DOI: 10.1115/1.4040415

[47] Ishaq M, Ali G, Shah Z, Islam S, Muhammad S. Entropy generation on nanofluid thin film flow of Eyring-Powell fluid with thermal radiation and MHD effect on an unsteady porous stretching sheet. Entropy. 2018;20(6): 412.
Available: https://doi.org/10.3390/e20060412

[48] Nasir S, Islam S, Gul T, Shah Z, Khan MA, Khan W, Khan AZ. Khan S. Three dimensional rotating flow of MHD single wall carbon nanotubes over a stretching sheet in presence of thermal radiation, Applied Nanoscience; 2018.
DOI: Doi.Org/10.1007/S13204-018-0766-0

[49] Muhammad S, Ali G, Shah Z, Islam S, Hussain SA. The rotating flow of magnetohydrodynamic carbon nanotubes over a stretching sheet with the impact of non-linear thermal radiation and heat generation/absorption. Appl. Sci. 2018;8(4):482.
DOI: 10.3390/app8040000

[50] Vafai K, Tien CL. Boundary and inertia effects on flow and heat transfer in porous media. International Journal of Heat and Mass Transfer. 1981;24:195-203.

[51] Raptis A. Radiation and free convection flow through a porous medium. Internal Journal of Communication in Heat and Mass Transfer. 1998;25: 289-295.

[52] Ingham DB, Pop I (Eds). Transport Phenomena in Porous Media. Oxford, Pergamon Press, Elsevier Science. 1998; II.

[53] Mohammadein AA, El-Amin MF. Thermal dispersion radiation effects on non-Darcy natural convection in a fluid saturated porous medium. Transport in Porous Media. 2000;40:153-163.

[54] Vafai K (Ed.). Handbook of Porous Media, Marcel Dekker, New York; 2000.

[55] Pop I, Ingham DB. Convective Heat Transfer: Mathematical and computational modelling of viscous fluids and porous media. Pergamon, Oxford; 2001.

[56] Ingham DB, Bejan A, Mamut E, Pop I (Eds.). Emerging technologies and techniques in porous media. Kluwer, Dordrecht; 2004.

[57] Ingham DB, Pop I (Eds.). Transport Phenomena in Porous Media. Elsevier, Oxford. 2005; III.

[58] Vafai K (Ed.). Handbook of Porous Media, Second Ed., Taylor and Francis, New York; 2000.

[59] Nield DA. Bejan A. Convection in Porous Media, Third Ed. Springer, New York; 2005.

[60] Hayat T, Abbas Z, Pop I, Asghar S. Effects of radiation and magnetic field on the mixed convection stagnation-point flow over a vertical stretching sheet in a porous medium. International Journal of Heat and Mass Transfer. 2010;53:466-474.

[61] Sajid M, Awais M, Nadeem S, Hayat T. The influence of slip condition on thin film flow of a fourth grade fluid by the homotopy analysis method. Computers and Mathematics with Applications. 2008; 56:2019-2026.

[62] Hayat T, Sajid M. Homotopy analysis of MHD boundary layer flow of an upper convected Maxwell fluid. International Journal of Engineering Science. 2007;45:393-401.

[63] Cogley ACL, Vincenti WG, Gilles ES. Differential approximation for radiative heat transfer in a non grey gas near equilibrium, American Institute of Aeronat. Astronaut. Journal. 1968;6:551–553.

[64] Heck A. Introduction to maple. Third Edition, Springer-Verlag, Germany; 2003.

Peer-review history:
The peer review history for this paper can be accessed here (Please copy paste the total link in your browser address bar)
http://www.sdiarticle3.com/review-history/43089